Plasmonics (2020) 15:849–859
https://doi.org/10.1007/s11468-019-01094-6

Near- and Far-Field Plasmonic Properties of Different Types of Eccentric Core-Shell Nanodimers

Gour Mohan Das[1] · Venkata Ramanaiah Dantham[1]

Received: 10 September 2019 / Accepted: 4 December 2019 / Published online: 18 December 2019

Abstract
Finite element method (FEM) simulations have been carried out on free-standing and finite dielectric substrate-supported eccentric (i) silica core-gold nanoshell dimers and (ii) gold core-silica nanoshell dimers for understanding their near- and far-field plasmonic properties. In the case of eccentric silica core-gold nanoshell dimers, multiple peaks are observed in the near- and far-field spectra due to the plasmon hybridization. The number of peaks is found to be sensitive to the core offset parameters of the nanoshells forming nanodimer. The wavelength locations of the peaks due to the constructive coupling of the lower order modes found relatively more sensitive to the dielectric substrate. The number of peaks in the near- and far-field spectra found the same presence and absence of the dielectric substrate. The values of full width at half maximum (FWHM) of the peaks observed in the near-field spectra are found larger as compared to those observed in the far-field spectra. In contrast, in the case of eccentric gold core-silica nanoshell dimers, multiple peaks have not been observed. The FWHM of the observed peak is found sensitive to the core offset parameters of the nanoshells, and the number of peaks in the near field- and far-field spectra found not same in the presence and absence of the dielectric substrate. Moreover, the differences in near- and far-field spectra of plasmonically coupled (i) concentric nanoshells, (ii) eccentric nanoshells, and (iii) concentric and eccentric nanoshells also investigated numerically.

Keywords Near-field · Far-field scattering · Eccentric core-shell nanodimer · Localized surface plasmon resonance · Finite element method · Multipolar plasmon modes · Finite dielectric substrate

Introduction

In the field of nanoplasmonics, concentric dielectric core-metal nanoshells have found useful for several applications [1–5]. The near-field and localized surface plasmon resonance (LSPR) wavelength of the nanoshells can be tuned easily by varying the radius, electric permittivity of the dielectric core as well as metal nanoshells, and thickness of the nanoshells [6–9]. For a few specific applications, bumpy nanoshells were used instead of smooth nanoshells due to the larger electric field that develops on the surface of the bumps [10, 11]. However, the bumps were found in random size and shape. Therefore, it was difficult to explain the experimentally observed results either with theoretical or numerical results [12].

Due to this reason, researchers have started using reduced symmetry core-shell nanoparticles or eccentric nanoparticles in which the inner dielectric core is displaced with respect to the center of the shell [13–21]. These kinds of nanoshells provide an additional degree of freedom to the researchers for tuning the LSPR wavelength just by varying the core offset [13–15]. In addition, giant near-field generates on its thin shell side [14–18]. These nanoshells were synthesized by Wang et al. for the first time, and core offset was controlled systematically using an anisotropic electroless plating technique [14]. These nanoshells were experimentally proved to be good candidates for surface-enhanced Raman spectroscopy, photothermal therapy of tumors, nanoscale optical sensing, and photothermal agents for selective killing of nosocomial and antibiotic-resistant bacteria [13–23].

The near- and far-field plasmonic properties of isolated and coupled concentric dielectric core-metal nanoshells were studied using quasi-static approach, finite element method (FEM), finite difference time domain (FDTD) method, and discrete dipole approximation (DDA) [8, 9, 24–26]. The role of dimensions, electric permittivity of the core and nanoshell, and nanoshell thickness on plasmonic properties was investigated systematically [6–9, 24–26]. In addition, numerical simulations were performed on isolated eccentric dielectric core-

✉ Venkata Ramanaiah Dantham
dantham@iitp.ac.in

[1] Department of Physics, Indian Institute of Technology Patna, Patna, Bihar 801103, India

metal nanoshells and reported the difference in plasmonic properties as compared with the isolated concentric nanoshells [13, 15, 18–21]. However, the near- and far-field plasmonic properties of plasmonically coupled free-standing and substrate-supported eccentric nanoshell dimers have not been explored. This motivated us to perform numerical investigation on eccentric dielectric core-metal nanoshell dimers.

In the case of metal core-dielectric nanoshells or shell protected nanoparticles, the metal cores are not exposed to the surroundings. Hence, the chemical stability of the metal cores becomes better, thereby improving the reproducibility of the experimental results. In case of experiments related to surface-enhanced fluorescence (SEF) technique, the dielectric nanoshells act as barriers between metal cores and fluorescent molecules and avoid direct contact, which leads to enhance non-radiative rates [27]. Therefore, the fluorescence of molecules kept in the vicinity of these kinds of nanoshells always enhances due to the enhancement of the radiative rates relative to the non-radiative rates. In case of solar cells, these kinds of nanoshells are better for increasing their performance and lifespan by protecting active metal cores from corrosive electrolytes [28, 29]. The concentric nanoshells can be synthesized easily using a standard Stöber method, and these nanoshells also found suitable candidates for imaging therapy [30–33] and for different catalytic applications [34]. Using wet chemistry methods, the eccentric metal core-dielectric nanoshells can also be synthesized [35–38], and these nanoshells are found suitable for different applications such as bioimaging and chemo-photothermal therapy [35], catalytic applications [36], light guiding, and switching [38]. It is important to note that the near- and far-field plasmonic properties of concentric and eccentric metal core-dielectric nanoshell dimers are not explored. This also motivated us to perform numerical investigation on these kinds of nanoshells.

Herein, we report (i) near- and far-field plasmonic properties of free-standing and substrate-supported concentric and eccentric dielectric (metal) core-metal (dielectric) nanoshell dimers; (ii) role of core offset parameter, thickness of the dielectric substrate, and refractive index contrast (RIC) at the boundary between nanodimer and substrate on the near- and far-field plasmonic properties; and (iii) difference in the spectra of plasmonically coupled (a) concentric nanoshells, (b) eccentric nanoshells, and (c) concentric and eccentric nanoshells.

Numerical Methodology

Recently, the numerical methods such as FEM, FDTD, and DDA have become efficient to reveal the near- and far-field plasmonic properties of simple as well as complex nanoplasmonic structures [24–26, 39, 40]. In many cases, the numerical results were used to explain the experimental results [14]. Therefore, the FEM was preferred in the present study. To perform numerical investigation on silica core-gold nanoshell dimers, four different geometries as shown in Fig. 1 were modeled in COMSOL Multiphysics 5.0 commercial software package, and the frequency domain FEM solver in RF module was used to study the plasmonic properties of the nanoparticles. For all the calculations, the values of core radius, shell radius, nanogap size, electric permittivity of the surrounding medium, and silica core were fixed at 38, 45, 4, 1.0, and 1.45 nm, respectively. The electric permittivity values of gold for different wavelengths were taken from Ref. 41. The top illumination geometry was used for all calculations. The electric field of the incident plane wave was always chosen as parallel to the dimer axis. The perfectly matched layer (PML) of suitable dimensions was used to eliminate undesired back reflections. The finite element mesh size was 1 nm for all simulations for better computational accuracy.

In general, the magnitude of the eccentricity of the non-concentric nanoshells is estimated from the core offset parameter (Ψ_{nsh}), which is a dimensionless quantity [15]. Physically, it helps us for the measurement of the movement of the core with respect to the center for an eccentric nanoshell. The expressions for core offset parameter of the nanoshells forming nanodimer are given below.

$$\psi_{nsh1} = \rho_1/(r_{sh1}-r_{c1}) \quad (1)$$

$$\psi_{nsh2} = \rho_2/(r_{sh2}-r_{c2}) \quad (2)$$

where Ψ_{nsh1} and Ψ_{nsh2} represent the core offset parameter in nanoshell 1 (nsh1) and nanoshell 2 (nsh2). ρ_1, r_{c1}, and r_{sh1} are the core offset, radius of the core, and shell in nsh1, respectively. ρ_2, r_{c2}, and r_{sh2} are the core offset, radius of the core, and shell in nsh2, respectively. In the case of symmetric and homogenous nanoshell dimer, $\Psi_{nsh1} = \Psi_{nsh2} = \Psi_{nsh}$, $\rho_1 = \rho_1 = \rho$, $r_{c1} = r_{c2} = r_c$, $r_{sh1} = r_{sh2} = r_{sh}$. Therefore, the above two expressions can be reduced as follows:

$$\psi_{nsh} = \rho/(r_{sh}-r_c) \quad (3)$$

In case of concentric nanoshell dimer, $\Psi_{nsh1} = \Psi_{nsh2} = 0$. It is to be noted that in nsh1, if the core shifts away from the nanogap, then Ψ_{nsh1} becomes negative. If it shifts close to the nanogap, then Ψ_{nsh1} becomes positive. However, in case of nsh2, the Ψ_{nsh2} becomes positive and negative when the core shifts away and close from the nanogap, respectively (Fig. 1). The near- [39] and far-field spectra [42] of free-standing nanoshell dimers were estimated by varying the values of Ψ_{nsh1} and Ψ_{nsh2}.

To study the plasmonic properties of metal (gold) core-dielectric (silica) nanoshell dimers, three geometries were modeled in COMSOL software (Fig. 2) and performed FEM simulations. The dimensions of the core and shell, nanogap size, and electric permittivity values of silica and gold were same as mentioned above. In these types of nanodimers also

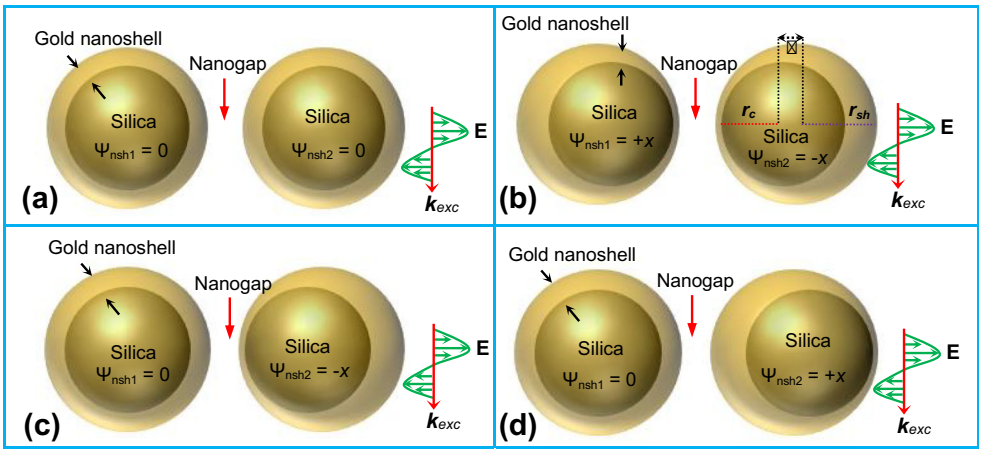

Fig. 1 Panel (a) shows an illustration of free-standing concentric dielectric (silica) core-metal (gold) nanoshell dimer. Panel (b) represents eccentric dielectric (silica) core-metal (gold) nanoshell dimer. Panels (c) and (d) represent coupled concentric and eccentric nanoparticle with negative and positive values of Ψ_{nsh2}, respectively

near- and far-field spectra were estimated by varying the core offset parameters in nsh1 and nsh2.

To study the role of refractive index contrast (RIC) at the boundary between nanoparticles and dielectric substrate (ξ) and thickness of the substrate on plasmonic properties of nanoshell dimers, two geometries were modeled in COMSOL (Fig. 3) and performed FEM simulations. Panel (a) shows an illustration of silica substrate-supported eccentric silica core-gold shell nanodimer. Panel (b) shows the silica substrate-supported eccentric gold core-silica nanoshell dimer. It is worth to mention here that in the literature, the role of ξ on optical properties of nanoplasmonic particles was reported by varying the electric permittivity of substrate. However, in the present study, the role of ξ on plasmonic properties was investigated by placing two different types of nanodimers on same dielectric substrate. To investigate the dependence of the thickness of the substrate (*t*) on plasmonic properties, the values of *t* were varied from 0 to 500 nm, and the diameter of the substrate was fixed at 2 μm.

Results and Discussion

Role of Core Offset Parameter on Near- and Far-Field Spectra of Free-Standing Eccentric Silica Core-Gold Nanoshell Dimer

Panels (a) and (b) of Fig. 4 show the near-field distribution of eccentric silica core-gold nanoshell dimer illuminated with two different excitation wavelengths. In both cases, the electric field is observed maximum at nanogap due to the constructive coupling of plasmon modes of both nanoshells forming nanoshell dimers. The maximum electric field (E_{ng}) values observed at nanogap for two different excitation wavelengths are in the order of 10^2 and 10^3. This clearly indicates the efficient excitation of plasmons at around 900 nm. The maximum electric field value at nanogap was estimated by taking line scan along the dimer axis. The near-field spectra of nanoshell dimer were calculated for different values of Ψ_{nsh1} and Ψ_{nsh2} using the procedure described in Ref. 35, and obtained

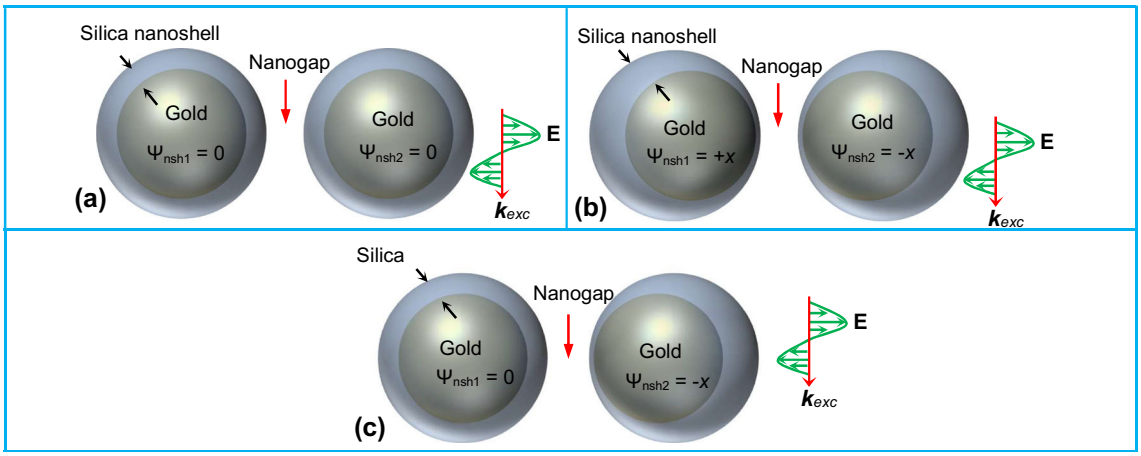

Fig. 2 Panel (a) shows an illustration of free-standing concentric metal (gold) core-dielectric (silica) nanoshell dimer. Panel (b) represents eccentric metal (gold) core-dielectric (silica) nanoshell dimer. Panel (c) represents coupled concentric and eccentric nanoparticle with negative value of Ψ_{nsh2}

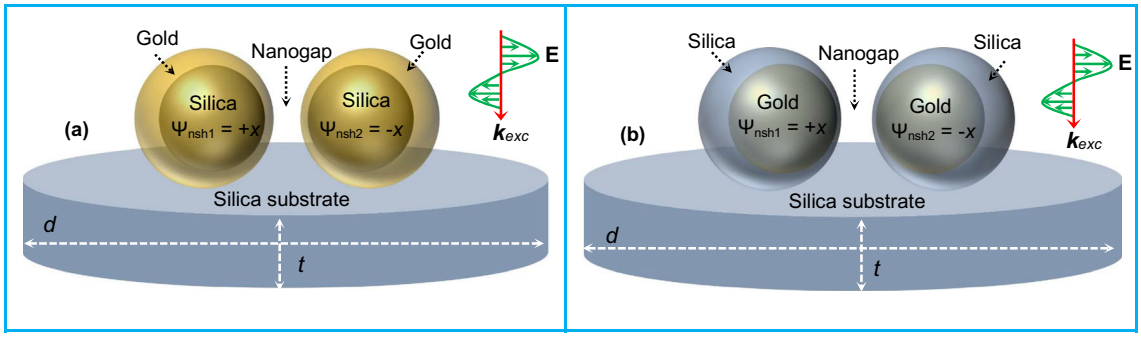

Fig. 3 Panels (a) and (b), respectively, show illustrations of eccentric dielectric core-metal nanoshell dimer and metal core-dielectric nanoshell dimer placed over a silica substrate. Here, t and d represent the thickness and diameter of the cylindrical dielectric (silica) substrate, respectively

spectra are shown in panel (c) of Fig. 4. From these spectra, we can conclude the following points: (i) in case of concentric nanodimer ($\Psi_{nsh1} = 0$ and $\Psi_{nsh2} = 0$), only one peak is observed in the near-field spectra due to the constructive coupling of dipole modes of primitive nanoshells; (ii) two peaks are observed in case of eccentric nanoshell dimer with $\Psi_{nsh1} = 0.69$ and $\Psi_{nsh2} = -0.69$ due to the constructive coupling of quadrupole and dipole modes of each nanoshell; and (iii) the number of peaks is found to increase with values of Ψ_{nsh1} and Ψ_{nsh2}, and this can be understood as follows.

According to the plasmon hybridization theory, the plasmon modes of each nanoshell of the nanodimer can be considered as the interaction between plasmons of a sphere and a cavity [15]. In the concentric nanoshells, multipoles of the primitive plasmon modes can interact only with modes of the same order: dipolar sphere modes hybridize only with dipolar cavity modes, for example. For the eccentric nanoshells, the selection rules of plasmon interaction are relaxed, allowing modes of different orders to hybridize. The high-order plasmon modes are often excited in the spectrum of the eccentric nanoshells [21]. The plasmon modes of the eccentric nanoshell dimers can be viewed as the combined results of two-level plasmon hybridization processes [19]. One is the hybridization of the primitive cavity mode (ω_c, $l = 1, 2, \ldots$) and

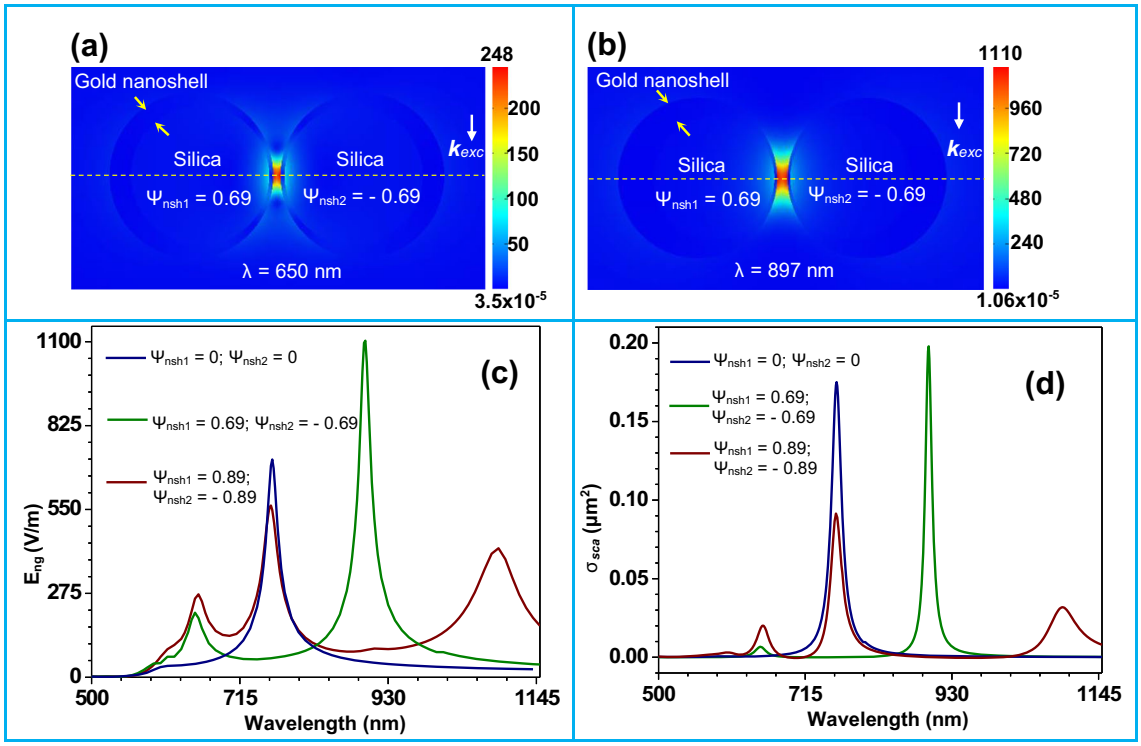

Fig. 4 Panels (a) and (b) show the near-field distribution of eccentric silica core-gold nanoshell dimer illuminated with plane wave of two different wavelengths. Panels (c) and (d) show the near- and the far-field spectra of free-standing silica core-gold nanoshell dimer with different values of Ψ_{nsh1} and Ψ_{nsh2}

Table 1 FWHM values of the plasmon modes observed in near- and far-field spectra of eccentric silica core-gold nanoshell dimer

(Ψnsh1, Ψnsh2)	λ_{mode} in nm	$(FWHM)_{near\text{-}field}$ in nm	$(FWHM)_{far\text{-}field}$ in nm
(0,0)	761.9	21	17
(0.69,-0.69)	650.2	35	21
	896.9	18	12
(0.89,-0.89)	653.8	35	25
	759.5	25	21
	1089.5	70	50

the sphere plasmon mode (ω_s, $l = 1, 2,\ldots$) of the eccentric nanoshell as explained above, and the other is the hybridization of the individual eccentric nanoshell plasmon modes ($l = 1, 2,\ldots$) of the dimer. Upon increasing the magnitude of ψ_{nsh1} and ψ_{nsh2} values, the hybridizations are expected to be enhanced. Due to this, the number of peaks increases in the near -and far-field spectra [19]. For different values of Ψ_{nsh1} and Ψ_{nsh2}, the number of plasmon modes and their wavelength locations in the far-field spectra (panel (d) of Fig. 4) is found to be nearly same as compared to those observed in the near-field spectra.

Table 1 shows the role of Ψ_{nsh1} and Ψ_{nsh2} on the full width at half maximum (FWHM) of the plasmon modes observed in near- and far-field spectra. From this table, it is clear that the FWHM values of the peaks are relatively larger in the near-field scattering spectra as compared to those observed in the far-field spectra. This clearly indicates that the optical losses in the near-field zone are larger than the far-field zone. In the case of the eccentric nanodimers, the FWHM of the peaks due to the lower order modes is found to increase with Ψ_{nsh1} and Ψ_{nsh2} values.

In order to investigate the near- and far-field spectra of plasmonically coupled concentric and eccentric silica core-gold nanoshells , two different systems [panels (c) and (d) of Fig. 1] were considered and performed FEM simulations. Panels (a) and (b) of Fig. 5 show the near-field distribution of coupled concentric and eccentric nanoshells illuminated with plane wave of wavelengths 837 and 759 nm, respectively. In both cases, the electric

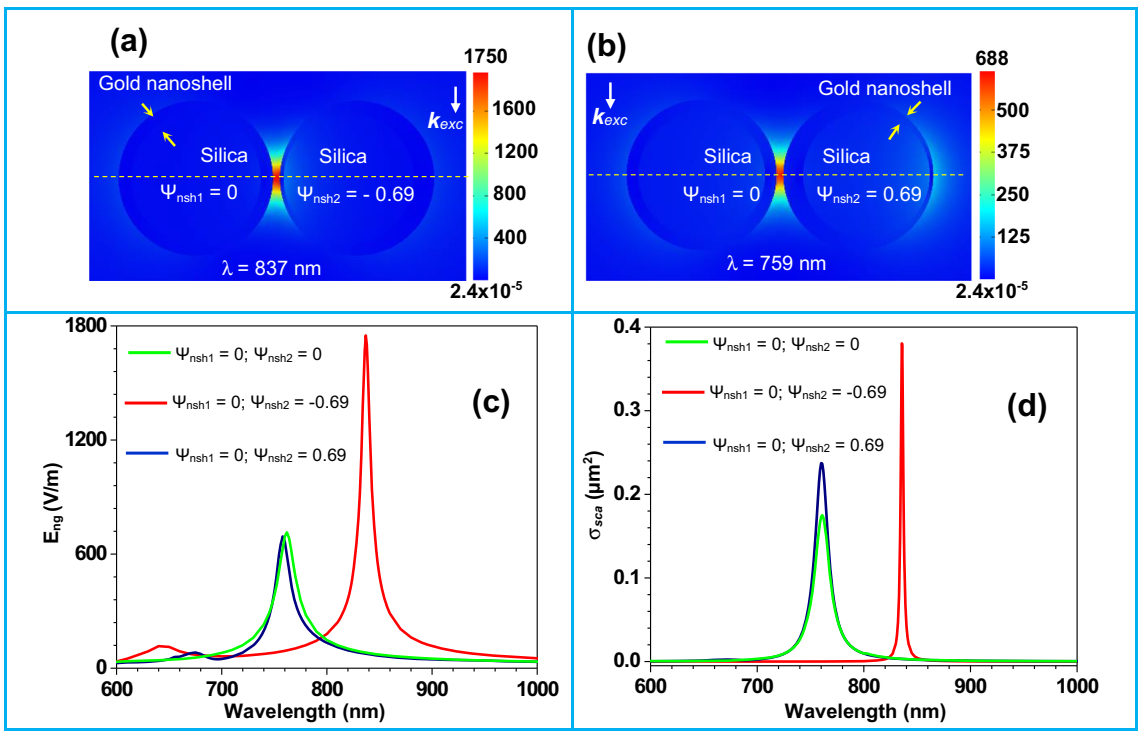

Fig. 5 Panels (a) and (b) show the near-field distribution of coupled concentric and eccentric silica core-gold nanoshells illuminated with plane wave of two different wavelengths. Panels (c) and (d) show the near- and far-field spectra of concentric silica core-gold nanoshell dimer and coupled concentric and eccentric silica core-gold nanoshells with different values of Ψ_{nsh2}, respectively

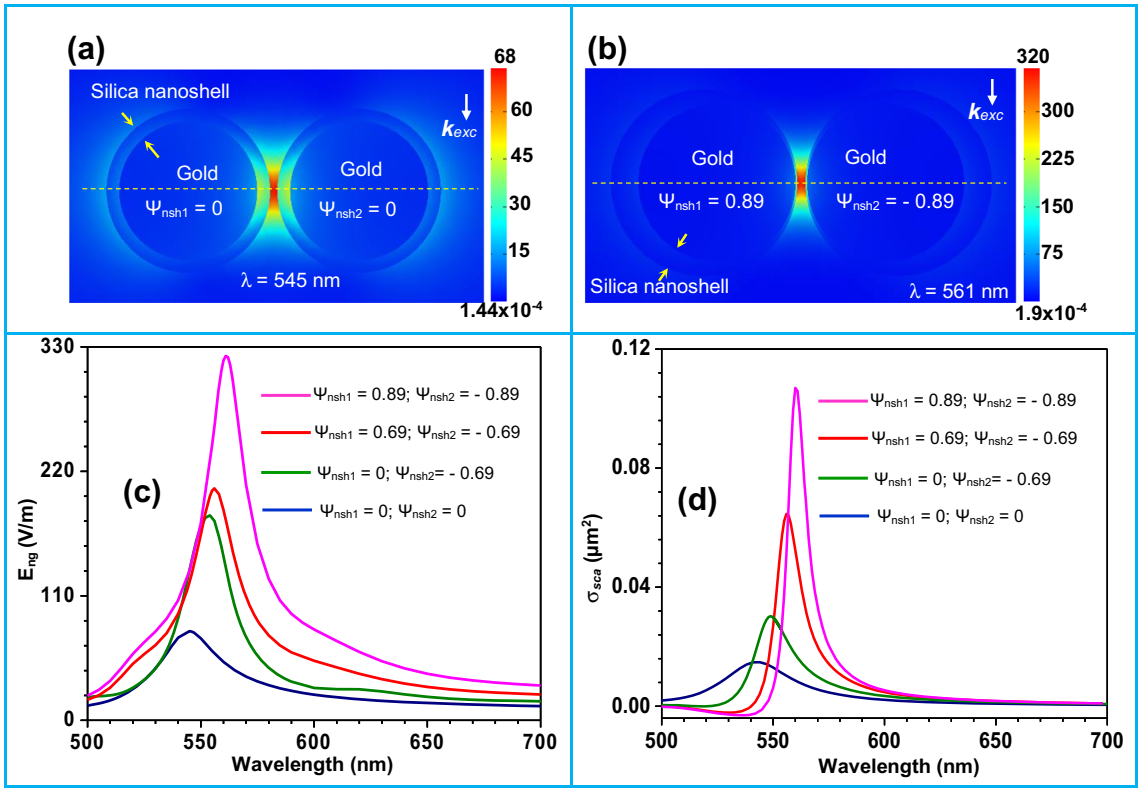

Fig. 6 Panels (a) and (b) show the near-field distribution of concentric and eccentric gold core-silica nanoshell dimer illuminated with plane wave of two different wavelengths. Panels (c) and (d), respectively, show the near- and far-field spectra of free-standing coupled gold core-silica nanoshells with different values of Ψ_{nsh1} and Ψ_{nsh2}

field is maximum at the nanogap due to the reason mentioned above. Panels (c) and (d) of Fig. 5 show the obtained near- and far-field spectra, respectively. From these figures, we can conclude the following points: (i) the intensity of the peaks originated due to the higher order plasmon modes is found to increase when Ψ_{nsh2} value is varied from 0 to +0.69. The intensity is found to increase further when Ψ_{nsh2} value is varied from +0.69 to −0.69. This clearly indicates that the higher order modes are relatively prominent in the eccentric nanoshell with negative core offset in nsh2. (ii) The separation between peaks is found to increase when the value of Ψ_{nsh2} is varied from 0 to +0.69, and this separation increases further when the value of Ψ_{nsh2} is varied from +0.69 to −0.69. (iii) Dipole mode is found prominent in the far-field scattering spectra for positive and negative values of Ψ_{nsh2}. (iv) Red shift in the wavelength location of the mode is observed in the far-field spectra when the Ψ_{nsh2} value is varied from 0 to −0.69. But significant change is not observed in the far-field spectra when the Ψ_{nsh2} value is varied from 0 to +0.69.

Role of Core Offset Parameter on Near- and Far-Field Spectra of Free-Standing Eccentric Gold Core-Silica Nanoshell Dimer

Panels (a) and (b) of Fig. 6 show the near-field distribution of free-standing concentric and eccentric gold core-silica nanoshell dimer illuminated with plane wave of wavelength of 545 and 560 nm, respectively. Here also, the value of electric field is maximum at the nanogap due to the reason mentioned above. The value of E_{ng} is five

Table 2 FWHM values of the plasmon modes observed in near- and far-field spectra of eccentric gold core-silica nanoshell dimer

(Ψnsh1, Ψnsh2)	λ_{mode} in nm	$(FWHM)_{near\text{-}field}$ in nm	$(FWHM)_{far\text{-}field}$ in nm
(0,0)	545.3	33	37
(0,0.69)	553.5	28	20
(0.69,-0.69)	556.1	22	14
(0.89,-0.89)	561.3	15	2

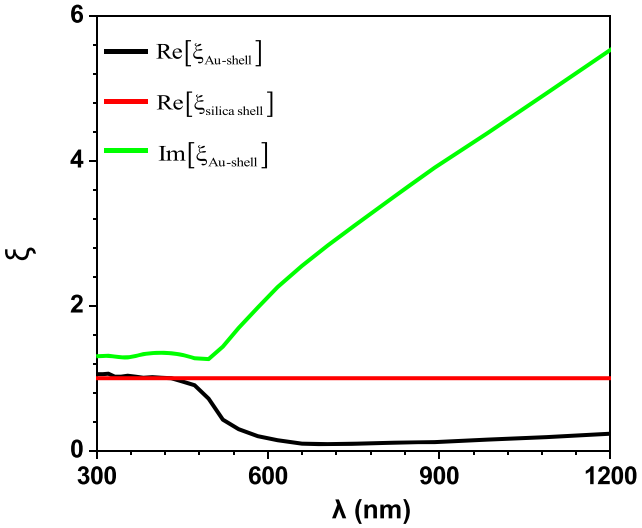

Fig. 7 The dependence of ξ on the values of λ

times larger in the case of eccentric nanoshell dimer due to the giant electric field on their thin shell side. Panels (c) and (d) show the near- and far-field spectra, and from these, we can conclude the following points: (i) in the case of eccentric gold core-silica nanoshell dimer, the value of E_{ng} is found to increase with the values of Ψ_{nsh1} and Ψ_{nsh2} which could be due to the enhancement of plasmon-plasmon coupling strength between two nanoshells. (ii) In contrast to the silica core-gold nanoshell dimers, only one peak is found in the near- and far-field spectra even though the values of Ψ_{nsh1} and Ψ_{nsh2} are varied from (0, 0) to (0.89, −0.89). This clearly indicates that there is no plasmon hybridization in eccentric gold core-silica nanoshell dimers. Numerical simulations were also carried out to understand plasmonic properties of isolated gold core-silica nanoshell by varying the core offset parameter value from 0 to 0.69 and found that there is no effect in the number of plasmon modes which indicates that there is no significant hybridization even in the individual eccentric nanoshells forming nanodimer. (iii) In both near- and far-field spectra, the FWHM of the peak is found to decrease upon increasing the values of Ψ_{nsh1} and Ψ_{nsh2}. (iv) Red shift in wavelength location of the peak is found upon increasing the values of Ψ_{nsh1} and Ψ_{nsh2}. (v) In the case of coupled concentric and eccentric nanoparticles, the value of E_{ng} and the magnitude of the shift are found to be larger as compared to those observed in the concentric nanoshell dimer.

Table 2 shows the role of Ψ_{nsh1} and Ψ_{nsh2} on the FWHM of the peaks observed in the near- and far-field spectra of gold core-silica shell nanodimer. From this table, it is clear that the FWHM values of the peaks are found to be significantly larger in the near-field spectra as compared to those in the far-field spectra.

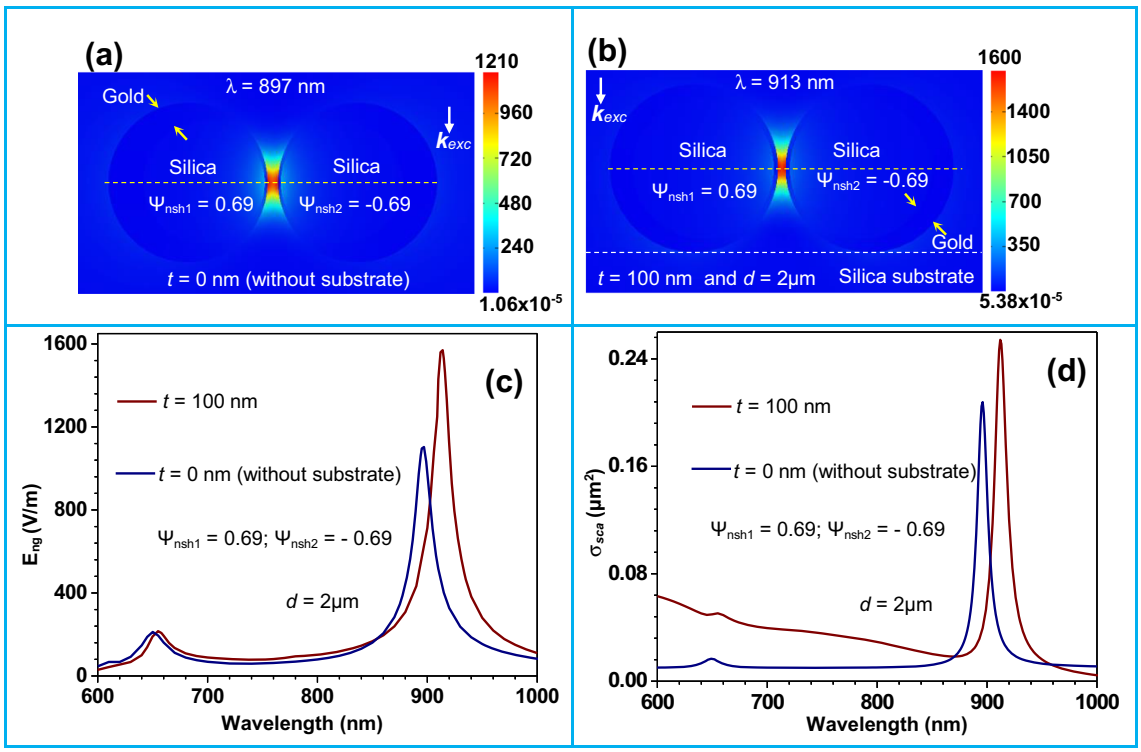

Fig. 8 Panels (a) and (b) show the near-field distribution of the free-standing and finite substrate-supported eccentric silica core-gold nanoshell dimer, respectively. Panels (c) and (d) show the role of t on near-field and far-field spectra of eccentric silica core-gold nanoshell dimer, respectively

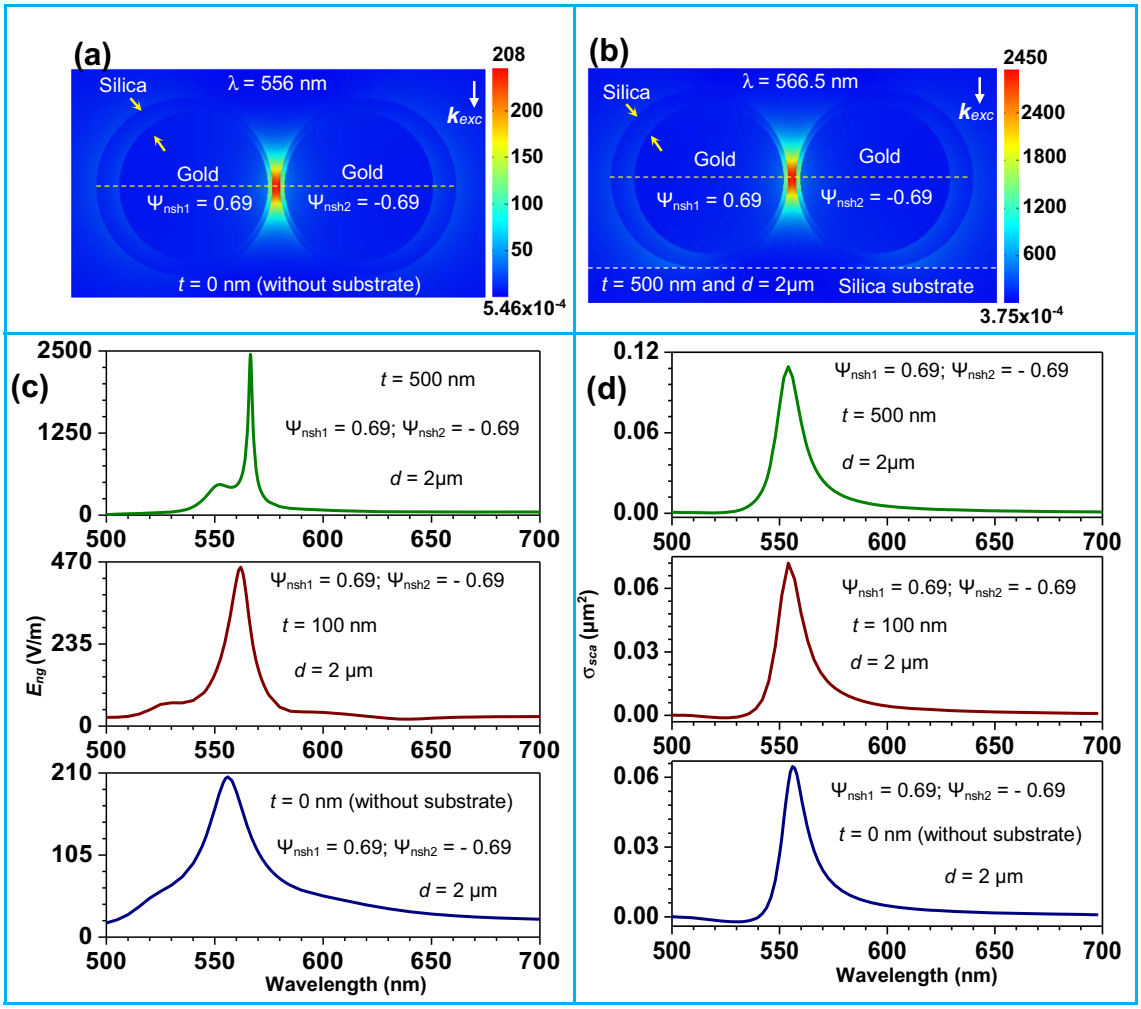

Fig. 9 Panels (a) and (b) show the near-field distribution of the free standing and finite substrate-supported eccentric gold core-silica nanoshell dimers, respectively. Panels (c) and (d) show the role of *t* on near- and far-field spectra of eccentric gold core-silica nanoshell dimers, respectively

Role of RIC at the Boundary Between Nanoshells and Finite Dielectric Substrate (ξ) on the Near- and Far-Field Spectra

In order to study the role of ξ on near- and far-field spectra, finite silica substrate-supported silica core-gold nanoshell and gold core-silica nanoshell dimers were chosen and performed FEM simulations. The expression of ξ is given by:

$$\xi = \frac{n_{shell} + i\, k_{shell}}{n_{sub} + i\, k_{sub}} \tag{4}$$

where n_{shell} and n_{sub} are the real part of the refractive indices of the shell and finite dielectric substrate, respectively. k_{shell} and k_{sub} are the imaginary part of the refractive indices of the shell and finite dielectric substrate, respectively. In the case of silica substrate-supported silica core-gold nanoshells, the RIC at the boundary between gold nanoshells and silica substrate ($\xi_{Au\text{-}shell}$) can be written as follows:

$$\xi_{Au-shell}(\lambda) = \frac{n_{Au}(\lambda) + ik_{Au}(\lambda)}{n_{silica} + ik_{silica}} \tag{5}$$

Since, the value of k_{silica} is very small as compared with n_{silica}, the value of k_{silica} can be ignored. Then the above equation reduces as follows:

$$\xi_{Au-shell}(\lambda) = \frac{n_{Au}(\lambda)}{n_{silica}} + i\frac{k_{Au}(\lambda)}{n_{silica}} = Re[\xi_{Au-shell}(\lambda)] + i\ Im[\xi_{Au-shell}(\lambda)] \tag{6}$$

where, the $Re[\xi_{Au\text{-}shell}]$ and $Im[\xi_{Au\text{-}shell}]$ are the real and imaginary parts of the $\xi_{Au\text{-}shell}$, respectively. The dependence of these values on λ is shown in Fig. 7. In the case of silica substrate-supported gold core-silica nanoshells,

$$\xi_{silica-shell} = \frac{n_{silica} + ik_{silica}}{n_{silica} + ik_{silica}} = 1 \tag{7}$$

The electric field distribution on the surface of free-standing and finite silica substrate-supported eccentric silica core-gold nanoshell dimer is shown in panels (a) and (b) of Fig. 8, respectively. It is observed that the value of E_{ng} is larger when the eccentric nanoshell is placed over a substrate. In both cases, the electric field is maximum at the nanogap between two nanoshells. Panels (c) and (d) of Fig. 8 show the near- and far-field spectra of free-standing and finite silica substrate-supported eccentric silica core-gold nanoshell dimer, respectively. From panel (a), it is clear that the peak originated due to the constructive coupling of lower order plasmon modes is red shifted in the presence of finite dielectric substrate. This indicates that the energy of the lower order modes of nanoshells forming dimer is reduced in the presence of the dielectric substrate due to the dielectric perturbation in the surrounding medium. However, the wavelength location of the peak originated due to the higher order modes of nanoshells is found slightly affected in the presence of the dielectric substrate. The possible reason for this is given below. The electric field values of the dipole and quadrupole decrease with the distance (r) away from the surface of the nanoshell as $1/r^3$ and $1/r^4$. So, the penetration depth of the dipole field is significantly larger in the substrate as compared with the quadrupole field. Due to this, the electric field of the dipole interacts with the dielectric substrate effectively as compared with the quadrupole and loses its energy significantly. In the case of far-field scattering spectra also, a peak originated due to the dipole mode of nanoshells is relatively found sensitive to the dielectric substrate.

The near-field distribution on the surface of free-standing and finite silica substrate-supported eccentric gold core-silica nanoshell dimer is shown in panel (a) and (b) of Fig. 9. The values of E_{ng} are in the order of 10^2 and 10^3 for excitation wavelengths of 556 and 566.5 nm, respectively. Panel (c) of Fig. 9 represents the near-field spectra of eccentric gold core-silica nanoshell dimer placed over silica substrate of different thickness. In these spectra, (i) the E_{ng} values are found to increase drastically with the t value as compared to that observed in the case of silica core-gold nanoshell eccentric dimer; (ii) all observed peaks are found to be sensitive to the dielectric substrate; and (iii) the red shift in wavelength locations of the peaks is observed upon increasing the t value. Panel (d) represents the far-field scattering spectra of eccentric gold core-silica nanoshell dimer placed over silica substrate of different thickness. In contrast to the substrate-supported eccentric silica core-gold nanoshell dimer, only lower order mode is found in the scattering spectra, and interestingly, wavelength location of the observed mode is found unaffected in the presence of the substrate of thickness ranging from 100 to 500 nm.

Conclusions

The FEM simulations have been carried out successfully on eccentric dielectric (metal) core-metal (dielectric) nanoshell dimers. In the case of concentric silica core-gold nanoshell dimers, one prominent peak has been observed in near- and far-field spectra due to the constructive coupling of lower order modes of nanoshells forming nanodimer. However, in the case of eccentric nanoshell dimers, multiple peaks (multipolar modes) have been observed due to the plasmon hybridization, and the number of multipolar modes has been found to increase in near- and far-field spectra with the increase of both Ψ_{nsh1} and Ψ_{nsh2}. In the case of free-standing eccentric gold core-silica nanoshell dimers, with the increase of Ψ_{nsh1} and Ψ_{nsh2} values from 0 to 0.89, the values of E_{ng} and σ_{sca} have been found to increase, and red shift has been observed in the wavelength locations of the plasmon modes. However, multipolar plasmon modes have not been observed even the values of Ψ_{nsh1} and Ψ_{nsh2} were increased from 0 to 0.89. Only the FWHM of the peaks has been found to decrease upon increasing the values of Ψ_{nsh1} and Ψ_{nsh2}. The plasmonic properties of coupled concentric and eccentric nanoshells have been found different as compared either with eccentric or concentric nanoshell dimer.

In the case of silica substrate-supported eccentric silica core-gold nanoshell dimers, the peak due to the constructive couple of lower order modes in nsh1 and nsh2 has been found sensitive to the dielectric substrate as compared with the peak due to the coupling of higher order modes. The near-field has been found to increase in the presence of the silica substrate. The number of peaks observed in the near- and far-field spectra has been found the same. In silica substrate-supported eccentric gold core-silica nanoshell dimers, the two peaks due to the coupling of lower and higher plasmon modes have been observed in the near-field spectra, and amplitude of the modes has been found to increase with the t value. The separation between the modes found to decrease with the value of t. In contrast, the higher order plasmon modes have not been observed in the far-field scattering spectra even the thickness of the substrate was varied from 0 to 500 nm. The FWHM of the peaks observed in both types of spectra has been found to be sensitive with the values of Ψ_{nsh1} and Ψ_{nsh2}. In all cases, the peaks observed in the near-field spectra have been found broader as compared to those observed in the far-field spectra. We believe that these observations will be useful to the researchers for optimizing the response of plasmonic devices based on dielectric (metal) core-metal (dielectric) nanoshells.

Funding Information The authors acknowledge the funding from Council of Scientific and Industrial Research (CSIR), Government of India, under Grant 03(1406)/17/EMR-II.

Compliance with Ethical Standards

Competing Interests The authors declare that they have no competing interests.

References

1. Loo C, Lowery A, Halas NJ, West JL, Drezek R (2005) Immunotargeted nanoshells for integrated cancer imaging and therapy. Nano Lett 5:709–711
2. Bikram M, Gobin AM, Whitmire RE, West JL (2007) Temperature-sensitive hydrogels with SiO_2–au nanoshells for controlled drug delivery. J Control Release 123:219–222
3. Gao Y, Li Y, Wang Y, Chen Y, Gu J, Zhao W, Ding J, Shi J (2005) Controlled synthesis of multilayered gold nanoshells for enhanced photothermal therapy and SERS detection. Small 11:77–83
4. Hirsch LR, Jackson JB, Lee A, Halas NJ, West JL (2003) A whole blood immunoassay using gold nanoshells. Anal Chem 75:2377–2381
5. Jain PK, El-Sayed MA (2007) Surface plasmon resonance sensitivity of metal nanostructures: physical basis and universal scaling in metal nanoshells. J Phys Chem C 111:17451–17454
6. Averitt RD, Westcott SL, Halas NJ (1999) Linear optical properties of gold nanoshells. J Opt Soc Am B 16:1824–1832
7. Hu Y, Fleming RC, Drezek RA (2008) Optical properties of gold-silica-gold multilayer nanoshells. Opt Express 16:19579–19591
8. Prodan E, Nordlander P, Halas NJ (2003) Electronic structure and optical properties of gold nanoshells. Nano Lett 3:1411–1415
9. Das GM, Dantham VR, Arya A (2019) Plasmonic properties of nano- and microscale dielectric substrates-supported nanoshell dimers: effects of type and propagation direction of excitation light. IEEE Photonics Journal 11:1–8
10. Kang H, Yang JK, Noh MS, Jo A et al (2014) One-step synthesis of silver nanoshells with bumps for highly sensitive near-IR SERS nanoprobes. J Mater Chem B 2:4415–4421
11. Chang H, Ko E, Kang H, Cha MG, Lee YS, Jeong DH (2017) Synthesis of optically tunable bumpy silver nanoshells by changing the silica core size and their SERS activities. RSC Adv 7:40255–40261
12. Rodríguez OP, Núñez PD, Iglesias VR, Priede LM, Rivera A, Pal U (2017) Near- and far-field optical response of eccentric nanoshells. Nanoscale Res Lett 12:1–7
13. Wu Y, Nordlander P (2006) Plasmon hybridization in nanoshells with a nonconcentric core. J Chem Phys 125:124708
14. Wang H, Wu Y, Lassiter B, Nehl CL, Hafner JH, Nordlander P, Halas NJ (2006) Symmetry breaking in individual plasmonic nanoparticles. Proc Natl Acad Sci 103:10856–10860
15. Knight MW, Halas NJ (2008) Nanoshells to nanoeggs to nanocups: optical properties of reduced symmetry core-shell nanoparticles beyond the quasistatic limit. New J Phys 10:105006
16. Hao F, Sonnefraud Y, Van Dorpe P, Maier SA, Halas NJ, Nordlander P (2008) Symmetry breaking in plasmonic nanocavities: subradiant LSPR sensing and a tunable Fano resonance. Nano Lett 8:3983–3988
17. Lal S, Grady NK, Kundu J, Levin CS, Lassiterde JB, Halas NJ (2008) Tailoring plasmonic substrates for surface enhanced spectroscopies. Chem Soc Rev 37:898–911
18. Moradi A (2009) Plasmon hybridization in metallic nanotubes with a nonconcentric core. Opt Commun 282:3368–3370
19. Yun B, Wang Z, Hu G, Cui Y (2010) Theoretical studies on the near field properties of non-concentric core-shell nanoparticle dimers. Opt Commun 283:2947–2952
20. Moradi A (2014) Surface plasmon modes of a nanoegg above a substrate. J Chem Phys 141:124121
21. Qian J, Sun YD et al (2015) Nanosphere-in-a-nanoegg: damping the high-order modes induced by symmetry breaking. Nanoscale Res Lett 10:1–8
22. Huang WC, Tsai PJ, Chen YC (2009) Multifunctional Fe_3O_4@au nanoeggs as photothermal agents for selective killing of nosocomial and antibiotic-resistant bacteria. Small 5:51–56
23. Cho WJ, Jung A, Han S, Lee SM, Kang T, Lee KH, Choi KC, Kim JK (2015) Plasmonic colloidal nanoparticles with open eccentric cavities via acid-induced chemical transformation. NPG Asia Materials 7:e167
24. Jain PK (2007) El-Sayed MA. Universal scaling of plasmon coupling in metal nanostructures: extension from particle pairs to nanoshells Nano Letters 7:2854–2858
25. Lombardi A, Grzelczak MP, Crut A, Maioli P, Pastoriza-Santos I, Liz-Marzán LM, del Fatti N, Vallée F (2013) Optical response of individual au–Ag@ SiO_2 heterodimers. ACS Nano 7:2522–2531
26. Oubre C, Nordlander P (2005) Finite-difference time-domain studies of the optical properties of nanoshell dimers. J Phys Chem B 109:10042–10051
27. Li JF, Lia CY, Aroca RF (2017) Plasmon-enhanced fluorescence spectroscopy. Chem Soc Rev 46:3962–3979
28. Törngren B, Akitsu K, Ylinen A, Sandén S, Jiang H, Ruokolainen J, Komatsu M, Hamamura T, Nakazaki J, Kubo T, Segawa H, Österbacka R, Smått JH (2014) Investigation of plasmonic gold-silica core-shell nanoparticle stability in dye-sensitized solar cell applications. J Colloid Interface Sci 427:54–61
29. N'Konou K, Many V, Ruiz CM, Delapierre MT, Torchio P (2018) Effect of shell thickness of gold-silica core-shell nanospheres embedded in an organic buffer matrix for plasmonic solar cells. J Appl Phys 123:063102
30. Liz-Marzan LM, Giersig M, Mulvaney P (1996) Synthesis of nanosized gold-silica core-shell particles. Langmuir 12:4329–4335
31. Vanderkooy A, Chen Y, Gonzaga F, Brook MA (2011) Silica shell/gold core nanoparticles: correlating shell thickness with the plasmonic red shift upon aggregation. ACS Appl Mater Interfaces 3:3942–3947
32. Moreiraa AF, Rodriguesa CF, Reisa CA, Costaa EC, Correia IJ (2018) Gold-core silica shell nanoparticles application in imaging and therapy: a review. Microporous Mesoporous Mater 270:168–179
33. Guarrotxena N, García O, Quijada-Garrido I (2018) Synthesis of au@ polymer nanohybrids with transited core-shell morphology from concentric to eccentric Emoji-N or Janus nanoparticles. Sci Rep 8:5721
34. Zhao Y, Yang D, Hu H, Chen L et al (2016) A simple approach to the synthesis of eccentric au@SiO_2 Janus nanostructures and their catalytic applications. Surf Sci 648:313–318
35. Han Q, Wang X, Sun Z, Xu X, Jin L, Qiao L, Yuan Q (2018) Rational design of Fe_3O_4@C nanoparticles for simultaneous bimodal imaging and chemo-photothermal therapy in vitro and in vivo. J Mater Chem B 6:5443–5450
36. Zhang L, Wang X, Zhang T, Liu C, Li D, Xing S (2019) Achieving Janus Ag@ N-doped carbon for oxygen reduction reaction from eccentric encapsulated Ag@ polypyrrole. J Alloys Compd 785:491–498
37. Yoon DK, Kumar A, Lee DG, Lee J, Kwon T, Choi J, Jin T, Shim JH, Lee IS (2019) Metal@ SiO_2 Core-shells with self-arrested migrating core. Nano Lett 19:3627–3633
38. Barreda ÁI, Gutiérrez Y, Sanz JM, González F, Moreno F (2017) Light guiding and switching using eccentric core-shell geometries. Sci Rep 7:11189
39. Hutter T, Mahajan S, Elliott SR (2013) Near-field optical enhancement by lead-sulfide quantum dots and metallic nanoparticles for SERS. J Raman Spectrosc 44:1292–1298

40. Das GM, Ringne AB, Dantham VR, Easwaran RK, Laha R (2017) Numerical investigations on photonic nanojet mediated surface enhanced Raman scattering and fluorescence techniques. Opt Express 25:19822–19831
41. Johnson PB, Christy RW (1972) Optical constants of the noble metals. Phys Rev B 6:4370–4379
42. Garcia-Etxarri A, Gómez-Medina R, Froufe-Perez LS, Lopez C, Chantada L, Scheffold F, Aizpurua J, Nieto-Vesperinas M, Sáenz JJ (2011) Strong magnetic response of submicron silicon particles in the infrared. Opt Express 19:4815–4826